Editors' Suggestion | Featured in Physics

Wrapping of Microparticles by Floppy Lipid Vesicles

Hendrik T. Spanke,[1] Robert W. Style,[1] Claire François-Martin,[1] Maria Feofilova,[1] Manuel Eisentraut,[2] Holger Kress,[2] Jaime Agudo-Canalejo,[3] and Eric R. Dufresne[1,*]

[1]*ETH Zürich, 8092 Zürich, Switzerland*

[2]*Department of Physics, University of Bayreuth, 95447 Bayreuth, Germany*

[3]*Max Planck Institute for Dynamics and Self-Organization (MPIDS), D-37077 Göttingen, Germany*

(Received 7 July 2020; accepted 13 October 2020; published 5 November 2020)

Lipid membranes, the barrier defining living cells and many of their subcompartments, bind to a wide variety of nano- and micrometer sized objects. In the presence of strong adhesive forces, membranes can strongly deform and wrap the particles, an essential step in crossing the membrane for a variety of healthy and disease-related processes. A large body of theoretical and numerical work has focused on identifying the physical properties that underly wrapping. Using a model system of micron-sized colloidal particles and giant unilamellar lipid vesicles with tunable adhesive forces, we measure a wrapping phase diagram and make quantitative comparisons to theoretical models. Our data are consistent with a model of membrane-particle interactions accounting for the adhesive energy per unit area, membrane bending rigidity, particle size, and vesicle radius.

DOI: 10.1103/PhysRevLett.125.198102

The interaction of nano- and microobjects with lipid membranes plays an important role in many biological processes. Examples range from the disease-related entry of viruses and bacteria into cells [1,2] to healthy docking and priming during vesicular trafficking [3]. The adhesion of membranes to curvature-stabilizing proteins, such as the BAR family, plays a central role in many membrane-shaping processes of eukaryotic cells [4–8]. Finally, nano- and microparticles can bind to membranes, acting as potential vectors for drug delivery [9].

The interaction of particles with membranes therefore has far-reaching consequences in biology and medicine. This has motivated a rich body of theoretical and computational physical models of membrane-particle interactions [10–21]. Some of the most basic questions revolve around the adhesion of individual particles with bilayer membranes. The simplest theory addressing this question considers the interaction of a spherical particle, of radius R_P, with an initially flat membrane connected to a constant tension reservoir [22]. Attractive forces driving adhesion are assumed to be short ranged, and are quantified by the adhesive energy per unit area, ω. Positive adhesion energies drive the membrane to wrap the particle. On the other hand, membrane deformation is resisted by its bending rigidity, κ_b, and tension, σ. These two membrane properties can be combined to create an important *bendocapillary* length scale, $\lambda_\sigma = \sqrt{\kappa_b/\sigma}$ [22]. At length scales smaller than λ_σ, membrane deformations are primarily resisted by bending energy, while at longer length scales, deformations are mainly opposed by tension. For low tension or small particles ($R_P \ll \lambda_\sigma$), wrapping is therefore governed by a balance of only adhesion and bending energy, captured by a second length scale, $\lambda_\omega = \sqrt{2\kappa_b/\omega}$. In that case, membranes should spontaneously wrap particles whenever $R_P > \lambda_\omega$ [10,22]. As tension increases, wrapping may require external forces for activation, and wrapped particles may partially unwrap or totally unbind from the membrane.

The assumption of a constant tension reservoir can break down when vesicles are sufficiently deflated, and have enough excess area to wrap a particle without fluctuations being hindered or the membrane being stretched. In that case, tension no longer plays a role and a pure competition between only bending and adhesion is recovered. Recent theoretical studies have shown that finite curvature of the membrane can be important for particle wrapping in this limit [23,24].

Recent experiments have begun to explore membrane-particle interactions, reviewed in Ref. [25]. While elucidating a range of higher-order phenomena, these experiments have not tested basic theories of adhesion. Experiments have either employed extremely strong irreversible interactions between particles and membranes [26–29], operated with very tense membranes where there is no significant membrane deformation at the single-particle scale [30,31], or worked with nanoparticles where the interaction between individual particles and membranes cannot be resolved [32].

In this Letter, we experimentally investigate the wrapping of micron-sized particles by giant unilamellar vesicles (GUVs) in the biologically relevant limit of low membrane tension and weak reversible adhesion. The interaction of particles and membranes is tuned continuously using the depletion effect. We observe three regimes of interaction between particles and membranes: nonwrapping,

spontaneous wrapping, and activated wrapping. In the latter case, an external force is required to drive a particle from an unwrapped state to its equilibrium wrapped state. Detailed comparison with theory suggests an essential role for membrane curvature.

Our model system consists of a dispersion of micron-sized polystyrene particles (1.08 ± 0.04 μm and 2.07 ± 0.03 μm in diameter) and GUVs in polymer solutions. The GUVs, consisting of 1-palmitoyl-2-oleyl-sn-glycero-3-phosphocholine (POPC) with 1% 1,2-dioleoyl-sn-glycero-3-phosphoethanolamine-N-(lissamine rhodamine B sulfonyl) (Rhodamine PE), are made by electroformation in a 280 mOsm/kg sucrose solution [33–35]. The osmolality of the solvent is adjusted through the addition of glucose (approximately 270 mM) to a slightly hypertonic value of 290 mOsm/kg. Over the course of hours, this slight osmotic imbalance drives the deflation of vesicles, leading to very low tensions, demonstrated in later sections.

To achieve tunable weak adhesion between particles and GUVs, we employ depletion interactions [30]. Generally, the depletion interaction between two objects has the form, $E_{ad} = \Pi \Delta V$ [36,37], where Π is the osmotic pressure of the depletant and ΔV is the change of the depletant's excluded volume due to contact. For low concentrations, n, of depletant, the osmotic pressure is well approximated with the ideal form, $\Pi = nk_BT$. The excluded volume, $\Delta V = -A_{\mathrm{co}}\ell$ where, ℓ is the range of range of the depletion interaction, and A_{co} is the contact area (i.e., the area over which the two surfaces are within depletion range of each other). Thus, the adhesion energy density, $\omega = -E_{ad}/A_{\mathrm{co}}$, has the form

$$\omega = n\ell k_BT \tag{1}$$

For hard sphere depletants, ℓ is expected to be equal to their diameter. For polymer depletants in a good solvent, $\ell \approx R_g$ [38]. As the depletion agent, we use polyethylene glycol (PEG) with a molecular weight of 10^5 g/mol, which has a radius of gyration R_g of about 16 nm, and an overlap concentration of 0.99 wt % [39,40]. We used a range of PEG concentrations between 0.14–0.65 wt % ($\pm$0.016 wt %) in the samples, yielding adhesion energies from 0.6 to 2.6 μJ/m^2. See the Supplemental Material for the exact sample composition [41]. In this range, micron-sized particles can strongly bind membranes while still enjoying reversible interactions with each of its constitutive lipid molecules.

The main challenge in using depletion interactions for studies of particle-vesicle adhesion is their nonspecificity. Depletion forces not only drive adhesion of particles to vesicles, but also the adhesion of vesicles to the surface of the sample chamber. At the depletion strengths used here, vesicles spread on flat glass surfaces. This significantly increases their tension, and usually leads to rupture [46], as shown in Supplemental Fig. S1. To suppress adhesion between vesicles and the walls of the sample chamber, we coat it with a loose network of poly(ethylene glycol) diacrylate (PEG-DA), described in the Supplemental Material. On this surface, adhesion is strongly reduced and vesicles remain floppy, even after sedimenting against the surface. An example of such a GUV, imaged with a confocal microscope, is shown in Figs. 1(a) and 1(b). As shown in Fig. 1(c), we hypothesize that the PEG-DA network is permeable to the depletion agent, reducing its effect.

With a robust mechanism for controlling the adhesion energy, we can now determine which conditions lead to the wrapping of particles by the membrane. The state of wrapping is easily inferred from fluorescent images of the particle and membrane. Figure 1(d) shows confocal micrographs of a 1.08 μm diameter fluorescent polystyrene particle in proximity to a fluorescently tagged GUV. In this

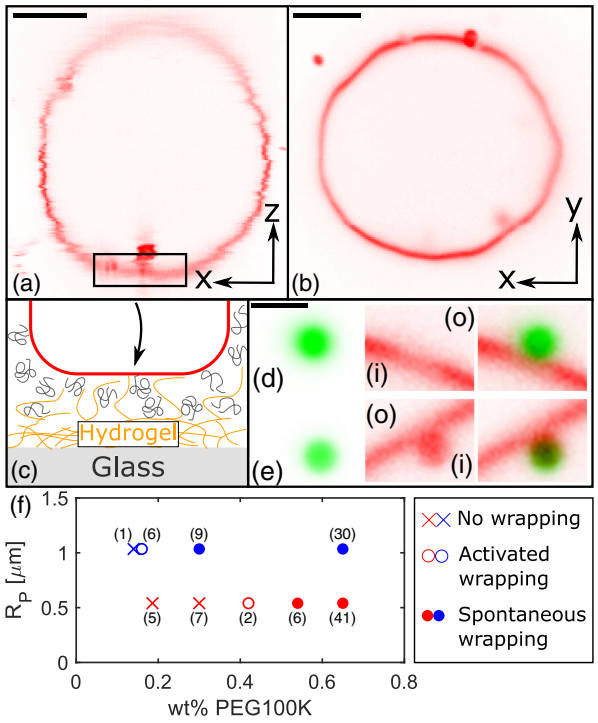

FIG. 1. Model system. (a),(b) Cross sections of a confocal image stack of a GUV sedimented on a PEG-DA hydrogel featuring obvious thermal fluctuations, despite the presence of 0.65 wt % PEG. Scale bars are 10 μm in length. (c) Schematic demonstrating a hypothesized mechanism for reduced depletion interactions against a hydrogel. (d),(e) Confocal images of 1.08 μm PS particles (green) and POPC membranes (red). The inside and outside of the GUV are indicated by "i" and "o," respectively. The particle in (d) with 0.24 wt % PEG100K does not deform the membrane. The membrane wraps the particle in (e) at 0.53 wt % PEG100K. The scale bar is 2 μm in length. (f) Empirical phase diagram based on the particle radius and amount of PEG depletant in the system. Numbers next to each data point indicate the number of membrane-particle pairs that were probed in each condition.

case, the particle is "unwrapped": the center of mass of the particle remains outside the convex hull of the GUV and there is no significant membrane deformation. By contrast, Fig. 1(e) shows a "wrapped" particle. Not only has the particle been pulled to the other side of the membrane's convex hull, but the membrane is strongly deformed and covers a large portion of the particle surface.

An empirical phase diagram showing the dependence of wrapping behavior on particle size and polymer concentration is shown in Fig. 1(f). To efficiently explore the interactions while minimizing unobserved membrane-particle binding events, we worked at low particle volume fractions $\phi < 10^{-5}$ and used optical tweezers to bring particles close to the GUV surface. At high polymer concentrations, we observe spontaneous wrapping of particles by membranes, shown by the filled circles in Fig. 1(f) (see Supplemental movie S1). At intermediate polymer concentrations, we observe activated wrapping, indicated by the open circles in Fig. 1(f). In this case, releasing a particle close to a GUV was insufficient to induce wrapping. Instead, wrapping could only be initiated by pushing the particle against the GUV with the optical tweezers. Nevertheless, particles remain stably wrapped after the laser was turned off (see Supplemental movie S2). At low polymer concentrations, there is no wrapping, as indicated by the x's in Fig. 1(f). In these cases, we can force the membrane to wrap a particle using optical tweezers. However, as soon as the trap is turned off, the membrane returns to its initial state and the particle diffuses away (see Supplemental movie S3). Note that the minimal polymer concentration needed to drive wrapping increases as the particle size decreases. This is qualitatively consistent with a simple competition of adhesion and bending rigidity, as summarized in the introduction. In that picture, activated wrapping should only occur at finite membrane tension [22].

The tension and bending rigidity of lipid bilayer membranes of individual vesicles, with radii R_V, can be extracted by an analysis of their thermal shape fluctuations [47–49]. For moderately tense vesicles, where $\lambda_\sigma \approx 0.1 R_V$, both the tension and bending rigidity can be reliably determined by comparing the mean amplitudes of the Fourier fluctuation modes to the expected Boltzmann distribution. λ_σ needs to be sufficiently small to ensure a reasonable number of fluctuation modes with a wavelength $\lambda > \lambda_\sigma$. This approach is called vesicle fluctuation analysis (VFA) and is summarized in the Supplemental Material [41]. Application of VFA to individual vesicles under the conditions in our experiments consistently reports $\kappa_b = 33 \pm 8 k_B T$ as shown in Supplemental Fig. S3. The resulting tensions are consistent with zero tension, with uncertainties varying from 10^{-9} to 10^{-7} N/m, shown in Supplemental Fig. S3.

To efficiently place an upper limit on the membrane tension for the vesicles used in the adhesion experiments, we inferred the most likely tension of the ensemble from simple measures of vesicle shape. We extracted the major and minor axes (a and b) of each GUV, just before it came into contact with the particle. Histograms of the mean vesicle radii, $R_V = (a/2 + b/2)/2$, and the normalized ellipticity $(a - b)/(a + b)$, are shown in Figs. 2(a) and 2(b). The vesicles' mean radii range from 5 to 25 μm and the normalized ellipticity varies from 10^{-3} to 0.55. Using a Monte Carlo simulation of vesicle fluctuations near equilibrium based on the same assumptions of VFA, described in the Supplemental Material, we calculated the probability distribution of the normalized ellipticities for a range of membrane tensions. Three probability distributions are shown in Fig. 2(c). The likelihood of each tension is determined by multiplying the probabilities of all the experimentally observed ellipticities. The log-likelihoods of tensions between 10^{-10} and 10^{-8} N/m are shown in Fig. 2(d). A tension of 3.2×10^{-10} N/m is the most likely tension to describe all GUVs observed.

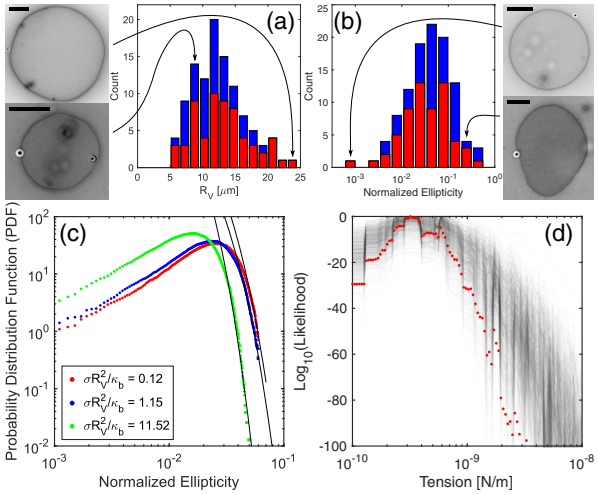

FIG. 2. Geometry and tension of GUVs (a),(b) Histograms of vesicle radii R_V, and normalized ellipticities. GUVs wrapping 0.54 and 1.04 μm radii particles are indicated in red and blue, respectively. The micrographs show examples of GUVs just before a spontaneous wrapping event. The scale bars are 10 μm in length. (c) Histogram of simulated ellipticities for reduced tensions, $\sigma R_V^2/\kappa_b = 0.12$, 1.15, 11.52. Black lines are exponential fits to the high-ellipticity tails. (d) Logarithm of the likelihood for a range of membrane tensions for the entire data set (red) and for 1000 randomly selected subsets of the data (light gray), each using half of the data set. Values have been shifted so that the most likely tension of each data set has a value of zero.

The VFA and maximum likelihood results show that tensions are very low, compatible with zero and comparable to the bending scale $\kappa/R_V^2 \approx 1.25 \times 10^{-9}$ N/m, suggesting that our vesicles are in the deflated, floppy regime. This is apparent from the strong deviations from sphericity observed [Fig. 2(b), movie S2]. As described in the introduction, in this regime the concept of an effective tension ceases to be useful and the system can be regarded as tensionless.

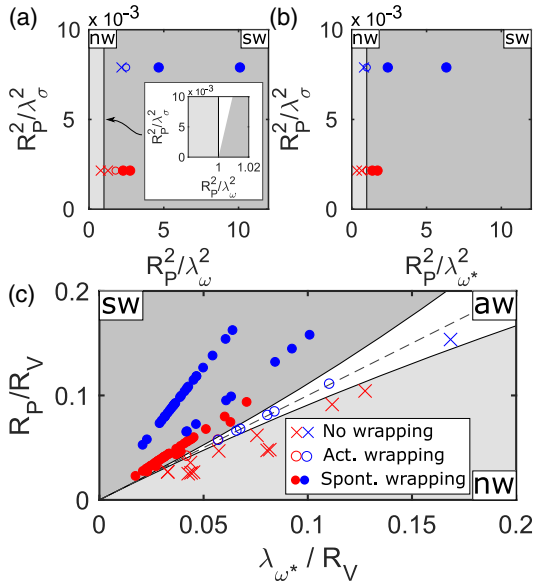

FIG. 3. Comparison of experiment and theory. (a) Phase diagram for flat membranes [22] compared to data from Fig. 1(f) using a membrane tension of 10^{-9} N/m and adhesion energy density ω from depletion [Eq. (1)]. Inset shows the narrow region of activated wrapping. Shading indicates theoretical predictions: dark gray for spontaneous wrapping (sw), light gray for non-wrapping (nw), and white for activated wrapping (aw). (b) Same with corrected adhesion energy density ω^* incorporating steric interactions [Eq. (2) and $c = 0.04$]. (c) Phase diagram for curved membranes [23] using the corrected adhesion energy density ω^* of Eq. (2) with $c = 0.04$.

Indeed, using 10^{-9} N/m as a representative value of tension, plotting our results in the theoretical phase diagram of [22] shows that, at such low tensions, the predictions are indistinguishable from those for a tensionless membrane [Fig. 3(a)]. The region of activated wrapping exists only in a tiny band around the boundary $R_P^2/\lambda_\omega^2 = 1$, see the inset of Fig. 3(a), corresponding to a difference in PEG concentration of 0.0023 wt %, which is much is smaller than our precision in defining the polymer concentration.

Furthermore, we find that we consistently need higher adhesion energies for spontaneous wrapping than predicted by the theory. This shift can be understood as a consequence of thermal fluctuations. Shape fluctuations increase the range of steric repulsions with a membrane, scaling like $1/x^2$, where x is the surface to surface separation [50]. For $x < \ell$, the net energy per unit area is

$$E(x)/A = -nk_BT(\ell - x) + c\frac{(k_BT)^2}{\kappa_b x^2}. \tag{2}$$

The first term captures the separation dependence of the depletion force. The second term is the steric repulsion and features an unspecified dimensionless constant c, predicted to be in the range of 0.01–0.23 [30,50]. Minimizing with respect to the separation, we find a reduced adhesion energy,

$$\omega^* = nk_BT\left[\ell - 3\left(\frac{ck_BT}{4n\kappa_b}\right)^{1/3}\right]. \tag{3}$$

Accounting for this additional repulsive interaction, we find a good fit between theory and experiments for the transition from free particles to activated wrapping using a value of $c = 0.04$ for both particle sizes, as shown in Fig. 3(b). Theory and experiment are consistent for a range of c from 0.028 to 0.055 (see Supplemental Material). These c values are also consistent with previous Monte Carlo simulations of membrane-solid wall repulsion, [51–53].

However, this correction for thermal fluctuations does not address the presence of a robust activated-wrapping regime. To understand this, we turn to recent theoretical advances on particle wrapping by deflated vesicles, for which membrane area and volume are conserved and tension does not play a role [23,24]. There, activated wrapping can occur when the membrane curves away from the particle at their point of initial contact, such as when a particle attaches to a GUV from the outside. The corresponding phase diagram is shown in Fig. 3(c). It is spanned by two variables, the relative size of the particle and the vesicle (R_P/R_V), and the relative size of the adhesion length scale and the vesicle (λ_ω/R_V). The transition from no wrapping (light gray) to activated wrapping (white) occurs at $R_P/R_V = 1/[1 + (\lambda_\omega/R_V)^{-1}]$. The transition from activated wrapping to spontaneous wrapping (dark gray) occurs at larger particles sizes, $R_P/R_V = 1/[(\lambda_\omega/R_V)^{-1} - 1]$. As vesicles become more strongly curved, the two transitions move further apart, broadening the range of adhesion energies where activated wrapping is expected. In the limit of low curvatures, the two transitions merge, and reduce to the result for a tensionless planar membrane of Ref. [22], $R_P/R_V = \lambda_\omega/R_V$, shown here as a dashed line. Superimposing the data from Fig. 1(f) on top of this phase diagram, we find good agreement. This theory can be expanded to incorporate nonzero spontaneous curvature, [23]. but this correction is not necessary to describe our data (see Supplemental Material) [41].

We have introduced a model system to probe the wrapping of spherical particles by lipid bilayer membranes featuring tunable adhesive interactions and low membrane tensions. Our experiments agree with theory accounting for the vesicle curvature and weakened depletion interactions due to thermal shape fluctuations. Our micron-scale experiments not only have clear connections to the interactions of microplastics with living cells [54,55], but they are also relevant to nanoscale interactions of proteins and lipid membranes. Like the latter case, our experiments are dominated by bending, i.e., $R_P \ll \lambda_\sigma$. Our experiments also start to probe regimes where the particle size is comparable to but smaller than the membrane radius of curvature, the typical regime for curvature stabilizing proteins. However, an isotropic sphere is a poor approximation for most folded

proteins. Additionally, many proteins do not simply adsorb to the membrane but also anchor themselves with hydrophobic tails. Despite these limitations, work on such model systems helps to establish the physical foundations for an understanding of membrane-particle interactions over a wide range of scales. Future studies should aim to clarify the nature of membrane-mediated particle interactions and the coupling of adsorption and self-assembly of particles to generate large-scale shape transformations of membranes.

We acknowledge helpful conversations with Raphael Sarfati, Patricia Bassereau, Karine Guevorkian, Markus Deserno, Rumiana Dimova, and Reinhard Lipowsky as well as funding from Grant No. 172824 of the Swiss National Science Foundation and the German Research Foundation (DFG)—Project No. 391977956—SFB 1357.

*eric.dufresne@mat.ethz.ch

[1] R. S. Flannagan, V. Jaumouill, and S. Grinstein, Annu. Rev. Pathol. Mech. Disease **7**, 61 (2012).
[2] S. Dasgupta, T. Auth, N. S. Gov, T. J. Satchwell, E. Hanssen, E. S. Zuccala, D. T. Riglar, A. M. Toye, T. Betz, J. Baum, and G. Gompper, Biophys. J. **107**, 43 (2014).
[3] T. Südhof, Neuron **80**, 675 (2013).
[4] T. Itoh, K. S. Erdmann, A. Roux, B. Habermann, H. Werner, and P. D. Camilli, Dev. Cell **9**, 791 (2005).
[5] Y. Kamioka, S. Fukuhara, H. Sawa, K. Nagashima, M. Masuda, M. Matsuda, and N. Mochizuki, J. Biol. Chem. **279**, 40091 (2004).
[6] H. T. McMahon and J. L. Gallop, Nature (London) **438**, 590 (2005).
[7] J. L. Gallop and H. T. McMahon, Biochemical Society Symposia **72**, 223 (2005).
[8] A. Frost, R. Perera, A. Roux, K. Spasov, O. Destaing, E. H. Egelman, P. D. Camilli, and V. M. Unger, Cell **132**, 807 (2008).
[9] S. Dasgupta, T. Auth, and G. Gompper, J. Phys. Condens. Matter **29**, 373003 (2017).
[10] R. Lipowsky and H.-G. Döbereiner, Europhys. Lett. **43**, 219 (1998).
[11] A. H. Bahrami, M. Raatz, J. Agudo-Canalejo, R. Michel, E. M. Curtis, C. K. Hall, M. Gradzielski, R. Lipowsky, and T. R. Weikl, Adv. Colloid Interface Sci. **208**, 214 (2014).
[12] S. Dasgupta, T. Auth, and G. Gompper, Nano Lett. **14**, 687 (2014).
[13] B. J. Reynwar, G. Illya, V. A. Harmandaris, M. M. Mller, K. Kremer, and M. Deserno, Nature (London) **447**, 461 (2007).
[14] A. H. Bahrami, R. Lipowsky, and T. R. Weikl, Phys. Rev. Lett. **109**, 188102 (2012).
[15] M. Raatz, R. Lipowsky, and T. R. Weikl, Soft Matter **10**, 3570 (2014).
[16] K. Xiong, J. Zhao, D. Yang, Q. Cheng, J. Wang, and H. Ji, Soft Matter **13**, 4644 (2017).
[17] I. Koltover, J. O. Rädler, and C. R. Safinya, Phys. Rev. Lett. **82**, 1991 (1999).
[18] T. Ruiz-Herrero, E. Velasco, and M. F. Hagan, J. Phys. Chem. B **116**, 9595 (2012).
[19] A. Šarić and A. Cacciuto, Phys. Rev. Lett. **108**, 118101 (2012).
[20] A. Šarić and A. Cacciuto, Soft Matter **9**, 6677 (2013).
[21] A. Vahid, A. Šarić, and T. Idema, Soft Matter **13**, 4924 (2017).
[22] M. Deserno, Phys. Rev. E **69**, 031903 (2004).
[23] J. Agudo-Canalejo and R. Lipowsky, ACS Nano **9**, 3704 (2015).
[24] A. H. Bahrami, R. Lipowsky, and T. R. Weikl, Soft Matter **12**, 581 (2016).
[25] T. Idema and D. J. Kraft, Curr. Opin. Colloid Interface Sci. **40**, 58 (2019), particle systems.
[26] C. Dietrich, M. Angelova, and B. Pouligny, J. Phys. II (France) **7**, 1651 (1997).
[27] C. van der Wel, A. Vahid, A. Šarić, T. Idema, D. Heinrich, and D. J. Kraft, Sci. Rep. **6**, 32825 (2016).
[28] R. Sarfati and E. R. Dufresne, Phys. Rev. E **94**, 012604 (2016).
[29] C. van der Wel, D. Heinrich, and D. J. Kraft, Biophys. J. **113**, 1037 (2017).
[30] A. D. Dinsmore, D. T. Wong, P. Nelson, and A. G. Yodh, Phys. Rev. Lett. **80**, 409 (1998).
[31] M. Wang, A. M. Mihut, E. Rieloff, A. P. Dabkowska, L. K. Månsson, J. N. Immink, E. Sparr, and J. J. Crassous, Proc. Natl. Acad. Sci. U.S.A. **116**, 5442 (2019).
[32] S. Zuraw-Weston, D. A. Wood, I. K. Torres, Y. Lee, L.-S. Wang, Z. Jiang, G. R. Lázaro, S. Wang, A. A. Rodal, M. F. Hagan *et al.*, Nanoscale **11**, 18464 (2019).
[33] M. I. Angelova and D. S. Dimitrov, Faraday Discuss. Chem. Soc. **81**, 303 (1986).
[34] M. I. Angelova, S. Soléau, P. Méléard, F. Faucon, and P. Bothorel, Preparation of giant vesicles by external ac electric fields. kinetics and applications, in *Trends in Colloid and Interface Science VI* (Steinkopff, Darmstadt, 1992), pp. 127–131, https://doi.org/10.1007/BFb0116295.
[35] R. Dimova and C. Marques, *The Giant Vesicle Book* (CRC Press, Boca Raton, FL, 2019).
[36] S. Asakura and F. Oosawa, J. Polym. Sci. **33**, 183 (1958).
[37] A. Vrij, Pure Appl. Chem. **48**, 471 (1976).
[38] R. Tuinier and H. N. W. Lekkerkerker, Eur. Phys. J. E **6**, 129 (2001).
[39] N. Ziebacz, S. A. Wieczorek, T. Kalwarczyk, M. Fiałkowski, and R. Hołyst, Soft Matter **7**, 7181 (2011).
[40] M. Rubinstein, R. H. Colby *et al.*, *Polymer Physics* (Oxford University Press, New York, 2003), Vol. 23.
[41] See Supplemental Material at http://link.aps.org/supplemental/10.1103/PhysRevLett.125.198102 for the exact sample composition, which includes Ref. [42], for details on the vesicle fluctuation analysis used, which includes Ref. [43], and for estimates of the spontaneous curvature in our system, which includes Refs. [44,45].
[42] C. L. Phillips, E. Jankowski, B. J. Krishnatreya, K. V. Edmond, S. Sacanna, D. G. Grier, D. J. Pine, and S. C. Glotzer, Soft Matter **10**, 7468 (2014).
[43] P. Méléard, T. Pott, H. Bouvrais, and J. H. Ipsen, Eur. Phys. J. E **34**, 116 (2011).
[44] Y. Liu, J. Agudo-Canalejo, A. Grafmller, R. Dimova, and R. Lipowsky, ACS Nano **10**, 463 (2016).

[45] M. Karimi, J. Steinkhler, D. Roy, R. Dasgupta, R. Lipowsky, and R. Dimova, Nano Lett. **18**, 7816 (2018).
[46] R. P. Richter, R. Brat, and A. R. Brisson, Langmuir **22**, 3497 (2006).
[47] A. F. Loftus, S. Noreng, V. L. Hsieh, and R. Parthasarathy, Langmuir **29**, 14588 (2013).
[48] H. Engelhardt, H. P. Duwe, and E. Sackmann, J. Phys. Lett. **46**, 395 (1985).
[49] J. F. Faucon, M. D. Mitov, P. Méléard, I. Bivas, and P. Bothorel, J. Phys. II (France) **50**, 2389 (1989).
[50] W. Helfrich and R. M. Servuss, Il Nuovo Cimento D **3**, 137 (1984).
[51] R. R. Netz and R. Lipowsky, Europhys. Lett. **29**, 345 (1995).
[52] G. Gompper and D. M. Kroll, Europhys. Lett. **9**, 59 (1989).
[53] W. Janke, H. Kleinert, and M. Meinhart, Phys. Lett. B **217**, 525 (1989).
[54] M. A. Browne, A. Dissanayake, T. S. Galloway, D. M. Lowe, and R. C. Thompson, Environ. Sci. Technol. **42**, 5026 (2008).
[55] N. von Moos, P. Burkhardt-Holm, and A. Khler, Environ. Sci. Technol. **46**, 11327 (2012).